HETEROCYCLES, Vol. 87, No. 2, 2013, pp. 275 - 301. © 2013 The Japan Institute of Heterocyclic Chemistry
Received, 6th November, 2012, Accepted, 21st November, 2012, Published online, 7th December, 2012
DOI: 10.3987/REV-12-758

DEVELOPMENT OF CARBAZOLE DYES FOR EFFICIENT MOLECULAR PHOTOVOLTAICS

Nagatoshi Koumura[1,2] and Kohjiro Hara[1]

[1] Research Center for Photovoltaic Technologies, National Institute of Advanced Industrial Science and Technology (AIST), Higashi 1-1-1, Tsukuba, Ibaraki 305-8565, Japan

[2] Graduate School of Pure and Applied Sciences, University of Tsukuba, Tenodai 1-1-1, Tsukuba, Ibaraki 305-8571, Japan

Abstract – Dye-Sensitized Solar Cells (DSSCs), which are one of the promising molecular photovoltaics, have been attracting considerable attention because the electrochemical solar cells exhibit high performance and potential for low-cost production. Dyes as photosensitizers are one of the most important components influencing the photovoltaic performances of DSSCs, because a photo-sensitizer determines the photoresponse range of the DSSC and initiates the primary steps of the photon absorption and the subsequent electron transfer process. Generally, Ru-polypyridyl-complex sensitizers, developed by Prof. Grätzel and coworkers, have been employed for efficient DSSCs. In addition to conventional Ru-complex sensitizers, metal-free organic dyes have also been utilized as sensitizers in DSSCs, and the photovoltaic performance of DSSCs based on organic-dye sensitizers has been improved relative to earlier studies of DSSCs with organic dyes. We have designed and synthesized alkyl-functionalized carbazole dyes to improve both solar-cell performance and long-term stability of the solar cells. Here, we report detailed syntheses of several sensitizers based on carbazole and carbazole derivatives donor part, and photovoltaic performances of DSSCs with these dyes.

CONTENTS

1. INTRODUCTION

Dye-sensitized solar cells (DSSCs) have been attracted much attention as the next candidates for the developing renewable energy sources due to the low cost production and relatively high solar energy conversion efficiency,[1] since Grätzel group achieved 7% of solar energy conversion efficiency in 1991 by using nano-porous titanium oxide electrodes, iodine redox in an electrolyte, and ruthenium complexes as sensitizers.[2] In recent years, over 11% of solar energy conversion efficiency for DSSCs have been reported,[3] and several types of solar modules in large area has been also developed from many manufactures for practical applications.As shown in Figure 1, DSSCs are consist of many materials, a transparent conductive oxide (TCO) electrode, a nano-porous titanium oxide, dyes molecules, electrolyte including redox materials, and platinum-coated TCO counter electrode, which are very important component for determining the photovoltaic performances of solar cells. A glass substrate coated by fluorine-doped tin oxides is typically used for the transparent conductive oxide electrodes because sintering at 500 ºC is required for a preparation of the titanium oxide with nano-porous structure on the electrodes. Recently, titanium oxide pastes, which can be sintered at relatively low temperature (around 120 ºC), have been developed,[4] and then DSSCs with a plastic substrate can be also fabricated. An iodine

as a redox and acetonitrile as an organic solvent are generally used in the electrolyte. In order to improve the solar cell stability, ionic liquids and/or high-boiling solvent such as 3-methoxypropionitrile are often used. In very recent, over 12% efficiency[5] of a DSSC based on the combination of porphyrin and organic dyes was reported using a cobalt complex redox in an electrolyte instead of iodine. Some additives such as lithium iodide (LiI), *t*-butylpyridine (TBP), and 1-methyl-3-propylimidazolium iodide (DMPImI) are also appropriately used to optimize the condition for the solar energy conversion efficiency.

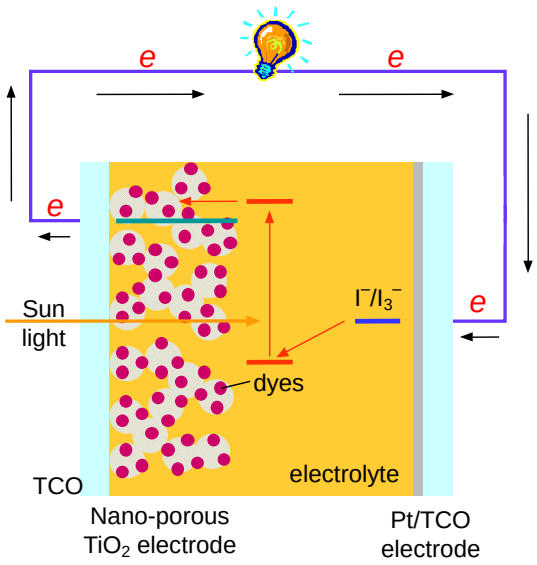

Figure 1. General structures of DSSCs

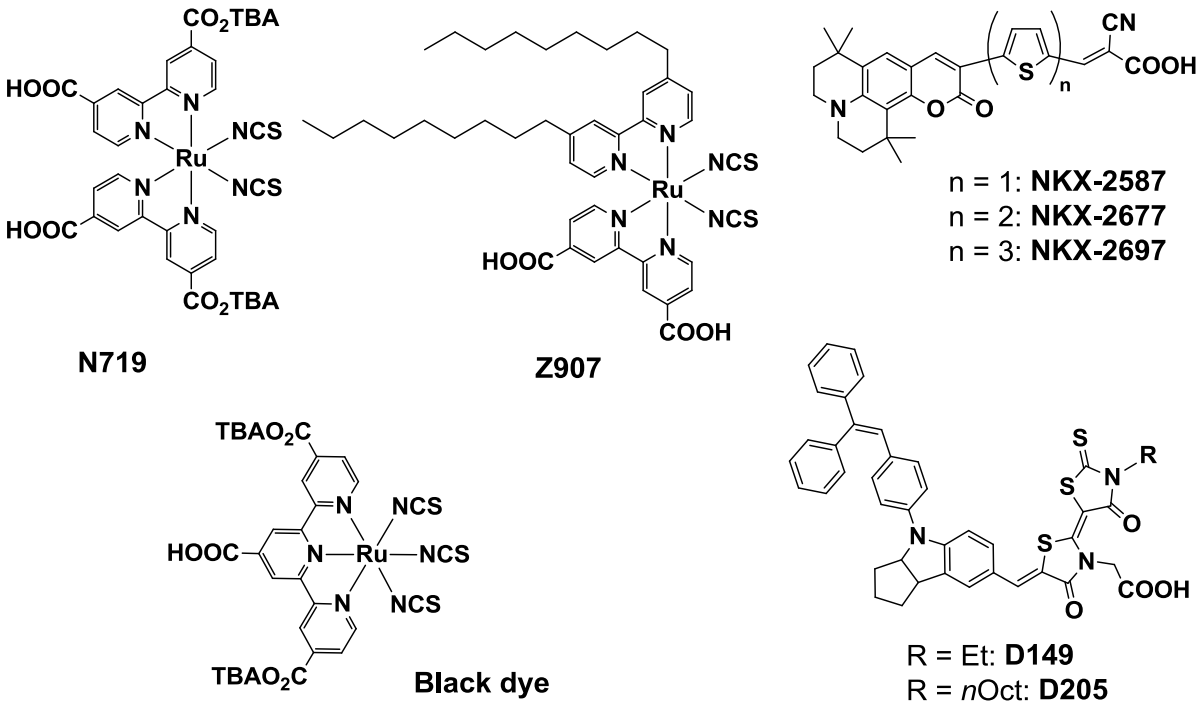

Figure 2. Examples of ruthenium dyes and organic dyes. TBA: tetra-*n*-butylammonium

Sensitizers are one of the most important components in determining the solar cell performance, because the light absorption of sensitizers is an initial process for the electron transfer in solar energy conversion mechanism and the spectral sensitivity of the solar cells can be determined by the absorption wavelength region of dyes. Ruthenium bi-pyridyl complexes, such as **N719**[6] and **Z907**,[7] and ruthenium ter-pyridyl complexes, black-dye,[8] are commonly used as sensitizers. Recently, many metal free organic dyes[9] have been designed and synthesized, for example, coumarin[10] (**NKX-2587**, **NKX-2677**, **NKX-2697** and so on) and indoline dyes[11] (**D149**, **D205** and so on), and then the solar energy conversion efficiency of DSSCs with these organic dyes has been greatly improved. The characteristics of organic dyes are mainly described as follows; (a) less-resource restriction, (b) high molar extinction coefficient by π-π* transition, (c) facile structural modification. However, photovoltaic performances of DSSCs based on organic dyes were observed to be low compared to those for DSSCs with ruthenium complex dyes. One of the possible reasons is the charge recombination from titanium oxide to tri-iodide ion in the electrolyte, and thereby decreasing open circuit voltages of DSSCs with organic dyes. Furthermore, an aggregation of these organic dye molecules often occurs due to the π-π stacking, which leads to the low electron injection yield from exited dye-molecules to titanium oxide. To prevent the dye-aggregation, a co-adsorbent, such as deoxycholic acid, is mostly mixed in a dye solution to improve the solar energy conversion efficiency of DSSCs based on organic dyes.

To overcome the above problems with the use of organic dyes into DSSCs while taking advantage of organic dyes, we have designed and synthesized novel carbazole dyes functionalized by alkyl chains on the oligothiophene linkage. Herein, we introduce the synthesis of the carbazole dyes and the photovoltaic performances of DSSCs with these carbazole dyes.

2. DESIGN AND SYNTHESIS OF CARBAZOLE DYES[12]

The common requirements of fundamental features of sensitizers for DSSCs are summarized as follows; (a) the efficient absorption property in a wide wavelength range, especially in visible region, (b) the optimal adjustment of HOMO-LUMO energy levels to the fermi-level of semiconducting titanium oxide and the electrolyte for a smooth electron transfer, (c) the existence of anchoring group(s) to be adsorbed on the titanium oxide surface. The light absorption property of organic dyes at long wavelength region has been achieved by the existence of donor-acceptor moieties connected by a π-electron conjugation in molecular structures. The HOMO-LUMO energy levels are mostly adjusted by the combination of donor and acceptor moieties. Aniline derivatives, such as triphenylamine, indoline and so on, as a donor, and a cyanoacrylic acid as an acceptor are generally used in dye-molecules for DSSCs. So we planned to apply

the carbazole moiety as a donor part of dye-molecules because of its robustness against external stimuli, such as heat and light, and a cyanoacrylic acid would be used as an acceptor and anchoring group, which has been conventionally used. Between the donor and acceptor, an oligothiophene unit was applied as an electron transfer part to obtain the light absorption property at long wavelength around visible region. Furthermore, we would introduce alkyl chains at the oligothiophene linkage for an additional function of dyes, which was the most important feature of the new dye structure, to overcome the problem of organic dyes as mentioned above. The molecular structures of new dyes are shown in Figure 3. The effects for the existence of alkyl chains in the dye-molecules would be expected as follows; (a) suppressing the dye-aggregation by π-π stacking, (b) preventing the approach of I_3^- ion to the TiO_2 surface by the steric hindrance of alkyl chains, (c) improvement of solar cell stability by diminishing the desorption of dye-molecules from the TiO_2 surface by the hydrophobicity of alkyl chains.

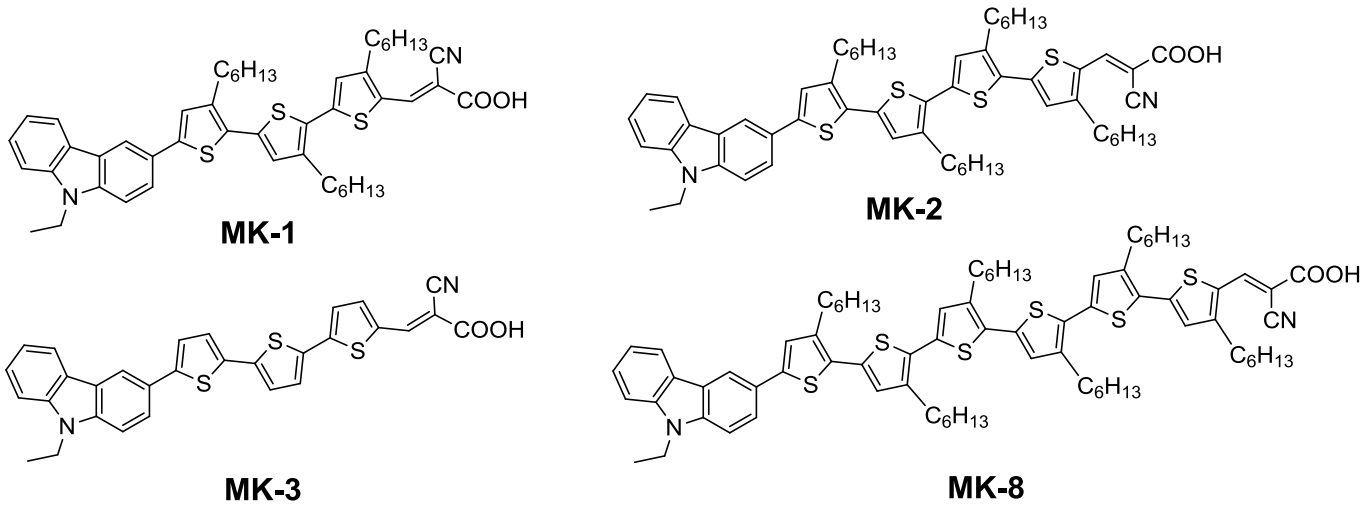

Figure 3. Molecular structures of MK dyes

As described in Scheme 1, these dyes were prepared from *N*-ethylcarbazole by the repeated bromination by *N*-bromosuccinimide (NBS) and Suzuki-Miyaura coupling reaction with 4-hexylthiophene-2-boronic acid neopentyl ester to construct the regio-regular oligothiophene moiety, and following the Vilsmeyer-formylation and the Knoevenagel condensation with a cyanoacetic acid. Mori et al. have reported another synthetic method for these dye-structures, which was the stepwise construction of oligothiophene moiety *via* the iterative palladium-catalyzed C-H arylation and halogen exchange reactions, as described in Scheme 2.[13] In addition, we also synthesized **MK-3** (in Figure 3), which has no alkyl chains at the oligothiophene part, in order to compare with these dyes (**MK-1** and **MK-2**).

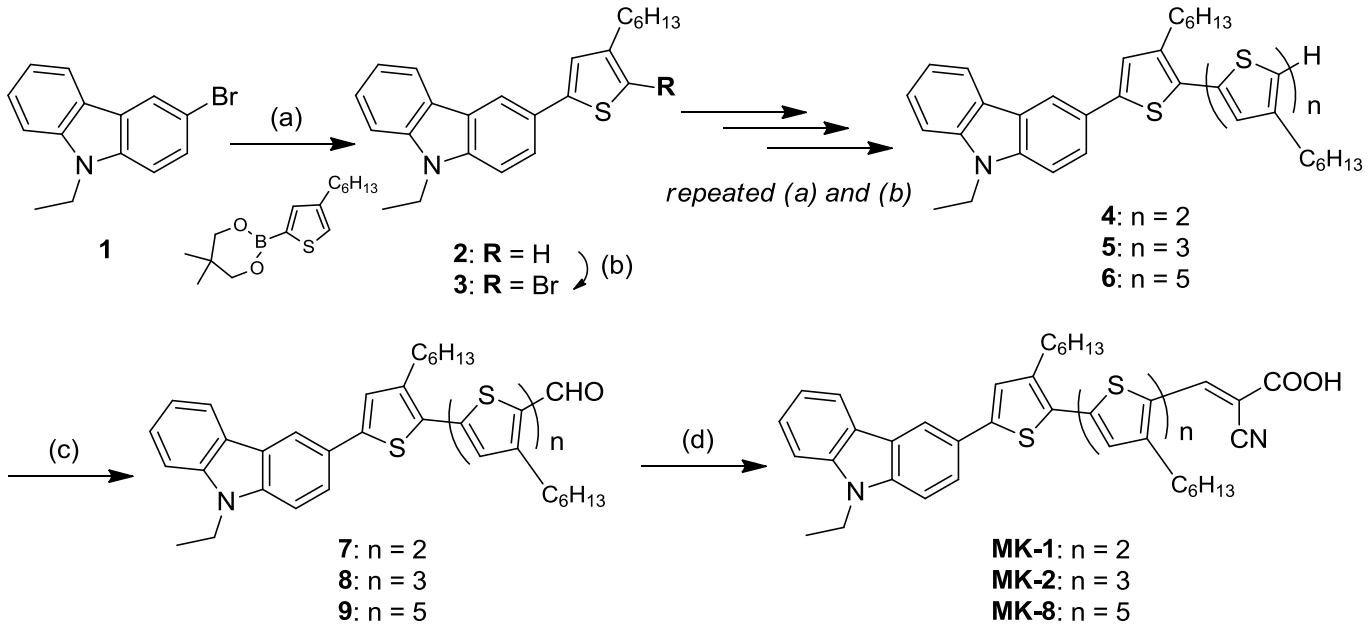

Scheme 1. Syntheses of **MK-1**, **MK-2** and **MK-8**; (a) 5,5'-dimethyl-2-(4-*n*-hexylthiophen-2-yl)-1,3,2-dioxaborinane, $Pd(PPh_3)_4$, Na_2CO_3aq/DME; (b) NBS/THF; (c) $POCl_3$-DMF/DMF; (d) cyanoacetic acid, piperidine /toluene-acetonitrile.

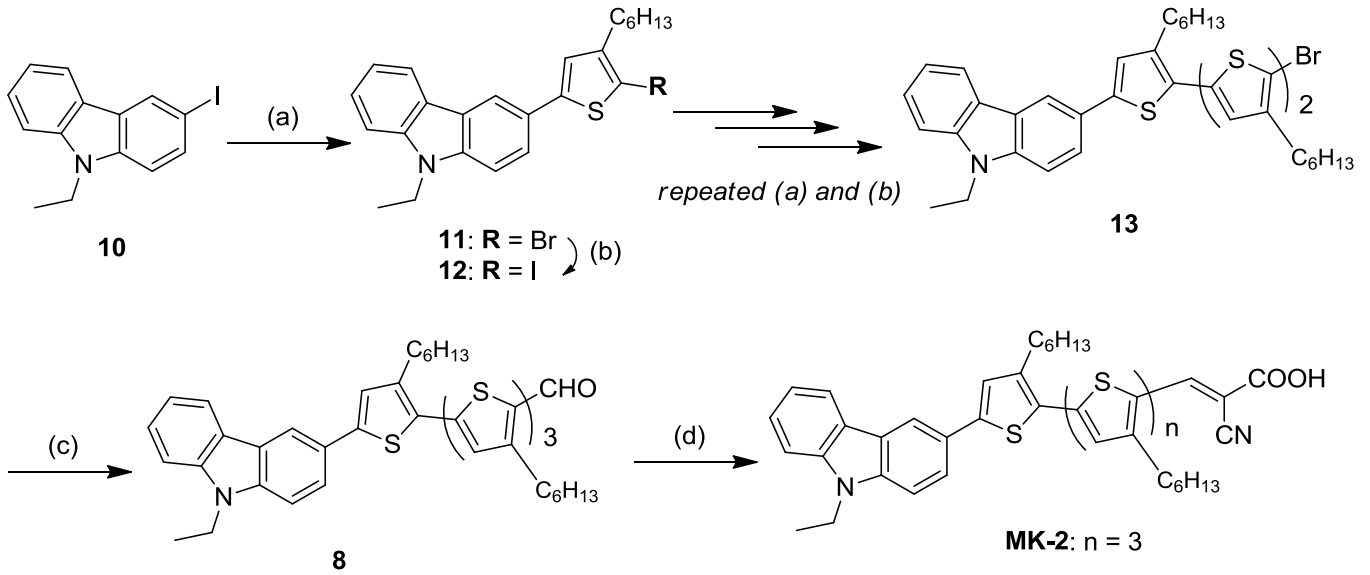

Scheme 2. Syntheses of **MK-2** *via* the iterative Pd-catalyzed C-H arylation and halogen exchange reaction; (a) 2-bromo-3-*n*-hexylthiophene, $PdCl_2(PPh_3)_2$, $AgNO_3$, KF/DMSO; (b) *n*-BuLi, I_2/THF; (c) 3-hexyl-5-iodothiophene-2-carbaldehyde, $PdCl_2(PPh_3)_2$, $AgNO_3$, KF/DMSO; (d) cyanoacetic acid, piperidine/toluene-acetonitrile.

3. ABSORPTION PROPERTIES OF MK DYES AND PHOTOVOLTAIC PERFORMANCES OF DSSCS BASED ON MK DYES[14]

3-1. Absorption and Electrochemical Properties of MK Dyes

The UV-vis absorption properties in 20%THF-toluene solution and the electrochemical properties of these dyes, **MK-1**, **MK-2**, **MK-3**, and **MK-8**, are depicted in Table 1. The absorption maxima (λ_{max}) around 480 nm of these dyes were observed due to the similar π-π* electron transition in the molecular structures. The molar extinction coefficient (ε) around 40,000 $M^{-1}\,cm^{-1}$ of dyes, **MK-1**, **MK-2**, and **MK-3** were observed, while 46,900 $M^{-1}\,cm^{-1}$ of ε for **MK-8** was observed due to the expansion of π-electron conjugation system. Figure 4a shows the UV-vis spectra of these dyes. The onset of these spectra for **MK-1**, **MK-2**, and **MK-8** are red-shifted with increasing the number of thiophene rings. Normalized UV-vis absorption spectra of dyes adsorbed on TiO_2 films are described in Figure 4b, and each λ_{max} for dye-loaded TiO_2 film is listed in Table 1. In comparison to the absorption properties in solution, the blue-shift of λ_{max} was observed in all cases of MK dyes, attributed to the deprotonation of the carboxylic acid.

As summarized in Table 1, the oxidation potentials (E_{ox}) of these dyes adsorbed on TiO_2 films (ca. 1.5 μm) were measured by the cyclic voltammetry and the reduction potentials (E_{red}) were calculated by the onset wavelength of the absorption spectra of these dyes on the TiO_2 films. The reduction potentials of all dyes are much more negative than the conduction band edge of TiO_2, which is located at –0.5 V (*vs.* NHE), and the oxidation potentials are sufficiently more positive than the iodine redox potential value (~0.4 V, *vs.* NHE). Therefore, the electron injection of the excited dye-molecules to the TiO_2 conduction band and the dye regeneration reaction from the electrolyte can smoothly occur.

Table 1. Absorption and electrochemical properties of MK dyes

Dye	λ_{max}[a] /nm (ε /$M^{-1}\,cm^{-1}$)	λ_{max}[b] /nm (on TiO_2)	E_{ox}[c] (V vs NHE)	gap[d] (V)	E_{red}[e] (V vs NHE)
MK-1	480 (38,800)	427	0.93	1.90	–0.97
MK-2	480 (38,400)	441	0.82	1.85	–1.03
MK-3	485 (40,100)	402	0.85	1.77	–0.92
MK-8	471 (46,900)	455	0.95	1.70	–0.75

[a] UV-vis spectrum of each dye was measured in a 20% THF-toluene solution through a 1 mm cell. [b] TiO_2 thickness ca. 1.5 mm. [c] Oxidation potentials of the dyes adsorbed on the TiO_2 films were measured under the following conditions: dye-adsorbed TiO_2 electrode (thickness: ca. 1.5 mm) as the working electrode, a Pt counter electrode, and a Ag /Ag+ reference electrode. Potentials measured *vs.* Fc /Fc^+ were converted to NHE by addition of +0.63 V, which were taken as E_{ox}. [d] Estimated from the onset wavelength of the absorption spectrum of dye-adsorbed TiO_2 electrode. [e] Calculated from the equation: $E_{red} = E_{ox}$ – gap.

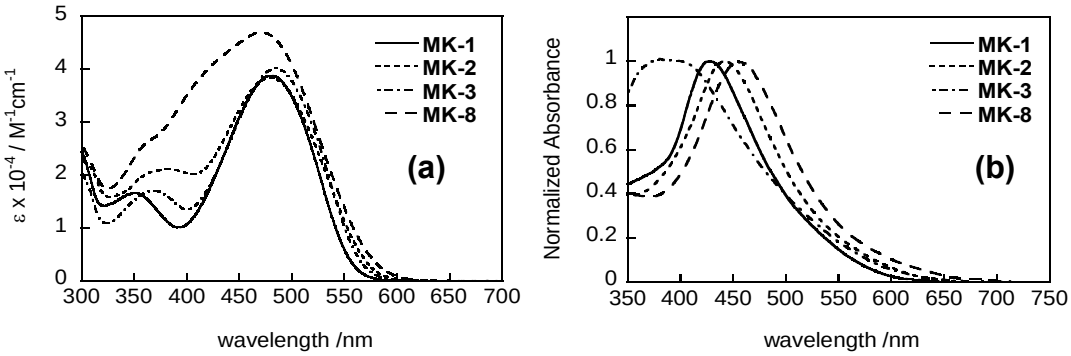

Figure 4. (a) UV-vis spectra of MK dyes in 20%THF-toluene; (b) UV-vis spectra of MK dyes on TiO_2 films.

3-2. Photovoltaic Performances of DSSCs based on MK dyes

The dye-adsorbed TiO_2 film electrode based on the fluorine-doped SnO_2 (FTO) coated glass substrate and Pt-coated FTO counter electrode were assembled into a sealed sandwich solar cell with a hot-melt Surlyn film (30 μm thickness) as spacer between the electrodes. Nanocrystalline TiO_2 electrodes, about 4 μm and 6 μm (transparent layer, consisting of ~20 nm nanoparticles) in thickness were prepared using screen printing technique. A drop of the electrolyte solution was put on the drilled hole in the counter electrode of the assembled cell. Finally, the two holes were sealed by the hot-melt Surlyn film covered with a thin slide glass. The electrolyte, 0.6 M DMPImI + 0.1 M LiI + 0.05 M I_2 + 0.5 M TBP in acetonitrile (AN), was employed to compare the photovoltaic performances of DSSCs between dyes.

Figure 5 shows action spectra of incident photon-to-current conversion efficiency (IPCE) for DSSCs based on MK dyes. The red-shift wavelength of IPCE spectra was observed with increasing the thiophene ring (**MK-1** < **MK-2** < **MK-8**) which is consistent with the tendency of UV-vis absorption spectra of dye-loaded TiO_2 films (Figure 4b), while a DSSC based on **MK-8** produced the IPCE maximum below 70%. The IPCE value around 75% were observed in the range of 400 to 650 nm with a maximum value of 75% at 480 nm for the DSSC based on **MK-2**, showing the highly efficient performance of the solar cells.

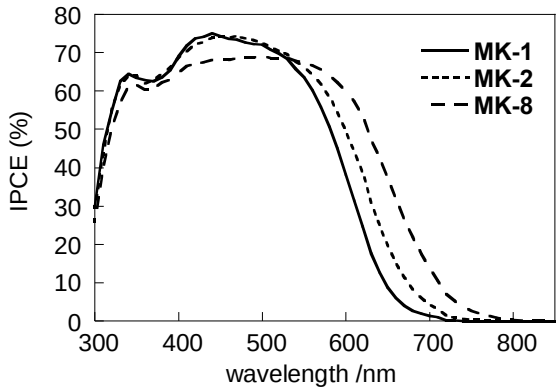

Figure 5. IPCE spectra of DSSCs based on **MK-1**, **MK-2**, and **MK-8**

Table 2. Photovoltaic Performances[a] of DSSCs based on **MK-1**, **MK-2**, **MK-3** and **MK-8**.

Dye	J_{SC} / mW cm^{-2}	V_{OC} / V	FF	η / %
MK-1	10.9	0.72	0.71	5.6
MK-2	12.4	0.72	0.71	6.3
MK-3	9.7	0.63	0.66	4.0
MK-8	12.5	0.72	0.68	6.1
MK-2[b]	15.2	0.72	0.75	8.3

[a] Incident light: AM 1.5G (100 mW cm^{-2}) with a mask and without an anti-reflection film, TiO_2 electrode: 6 μm, Cell area: 0.2354 cm^2, Electrolyte: 0.6 M DMPImI + 0.1 M LiI + 0.05 M I_2 + 0.5 M TBP in acetonitrile, [b] TiO_2 electrode: 16 μm, Cell area: 0.2354 cm^2, Electrolyte: 0.6 M DMPImI + 0.1 M LiI + 0.2 M I_2 + 0.5 M TBP in acetonitrile.

The photovoltaic performances of DSSCs based on these dyes are summarized in Table 2. The short current density (J_{SC}) increased in the order of **MK-1** < **MK-2** < **MK-8** as a result of the broader of IPCE action spectra with increasing the number of thiophene rings. If the maximum IPCE of **MK-8** based DSSC was comparable to that of **MK-2** based DSSC, the J_{SC} for a DSSC/**MK-8** should be much higher than the observed data. Note that the open circuit voltage (V_{OC}), 0.72 V, for DSSCs based on **MK-1**, **MK-2**, and **MK-8**, which have long alkyl chains, were observed higher than that for **MK-3**, 0.63 V, in the same condition. To improve the photovoltaic performances of DSSCs with organic dyes, in general, co-adsorbents, such as chenodeoxycholic acid, are commonly used in mixed solution with dye at the preparation of the dye-loaded TiO_2 electrode. Because in this work we have never used any co-adsorbent, it is indicated that these new dyes with *n*-hexyl chains at the oligothiophene linkage have functions as not only photo-sensitizer but also co-adsorbent in the dye-molecular. In other words, we found that the interfacial engineering of dye-adsorbed TiO_2 surfaces could be controlled by the structural modification of dye-molecule to achieve the high photovoltaic performance of organic dye sensitized solar cells.

Among the DSSCs based on the dyes, as the result of the optimization of the TiO_2 thickness and electrolyte, DSSC/**MK-2** showed the best conversion efficiency of 8.3% (J_{SC} = 15.2 mA cm^{-2}, V_{OC} = 0.73 V, FF = 0.75) under one sun condition when the TiO_2 electrode, 16 μm in thickness (consisting of a 9 μm transparent layer (~20 nm nanoparticles) and a 7 μm scattering layer (70% of nanoparticles and 30% of large-size particles (~100 nm))) was prepared, and the iodine content was increased from 0.05 to 0.2 M. It could be considered that J_{SC} and fill factor (FF) were generally improved but V_{OC} was decreased at the high concentration of iodine in the electrolyte due to the charge recombination from TiO_2 to I_3^-. In our

case, since the relatively high V_{OC} value was observed for DSSCs with **MK-2**, the charge recombination could be suppressed by the blocking effect of long alkyl chains in the dye-molecules.

To understand the result of high open circuit voltage for DSSCs based on MK dyes with long alkyl chains, we measured electron lifetimes (τ) in the conduction band of TiO_2. As shown in Figure 6, it is noteworthy that the value of τ for the DSSCs with **MK-1** and **MK-2** were longer than those with coumarin dyes, NKX2587 and NKX-2697, which have an oligothiophene linkage without alkyl chains. In addition, the t for the DSSC based on MK-3, having no alkyl chains, was much shorter than those with **MK-1** and **MK-2**. This result indicates that the existence of alkyl chains are remarkably effective in increasing the electron lifetime. The reason for the long electron lifetimes of DSSCs with MK dyes can be realized by the possibility that the hexyl chains act as a blocking layer preventing I_3^- ion approaching to the TiO_2 surface.

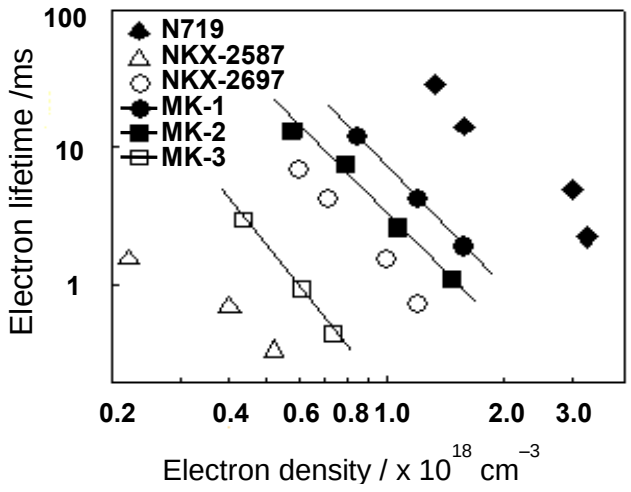

Figure 6. Electron lifetime in DSSCs based on various organic dyes as a function of electron density in DSSCs.

4. SUBSTITUTED CARBAZOLE DYES FOR DSSCS

4-1. Synthesis and Absorption Properties of Substituted Carbazole Dyes[15]

We designed and synthesized substituted carbazole dyes, **MK-14** and **MK-16**, which have a hexyloxyphenyl substituent on the carbazole moiety in the opposite side of an oligothiophene linker. Our strategy of the molecular design for these dyes was based on two concepts: a further retardation of charge recombination by the additional long alkyl chain in the donor part, and an extension of absorption wavelength by increasing the donor ability. **MK-14** and **MK-16** were prepared from 3-bromo-9-ethylcarbazole as described in Scheme 3. Oligothiophene moieties were constructed by the

repeating Suzuki coupling and bromination, and following the Vilsmeyer-formylation and the Knoevenagel condensation with a cyanoacetic acid, as well as the syntheses of **MK- 1** and **MK-2**. Figure 7 shows UV-vis spectra of **MK-14** and **MK-16** in 20%THF-tolunene solution. The absorption maxima and molar extinction coefficients (around 480 nm and 38,000 $M^{-1}cm^{-1}$) of these dyes were similarly observed as those of **MK-1** and **MK-2**. The onset of UV-vis spectra of **MK-14** (612 nm) and **MK-16** (622 nm) slightly red-shifted in comparison to those of **MK-1** (600 nm) and **MK-2** (619 nm), which could be due to the increasing donor ability of carbazole moiety.

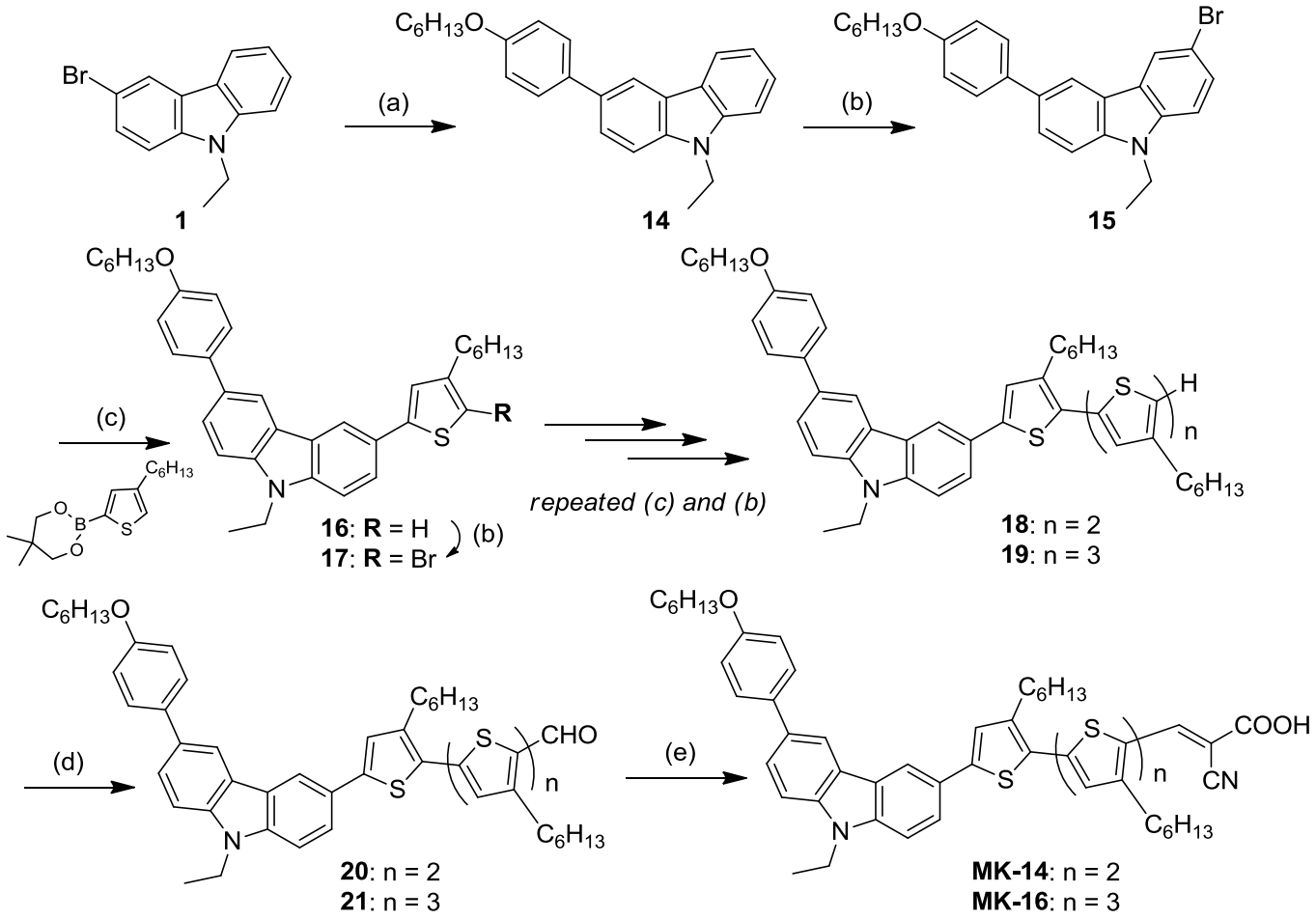

Scheme 3. Syntheses of **MK-14** and **MK-16**; (a) (i) 1-bromo-4-(hexyloxy)benzene, Mg/THF; (ii) $NiCl_2$(dppp)/THF; (b) NBS/THF; (c) 5,5'-dimethyl-2-(4-*n*-hexylthiophen-2-yl)-1,3,2-dioxaborinane, $Pd(PPh_3)_4$, Na_2CO_3aq/DME; (d) $POCl_3$-DMF/DMF; (e) cyanoacetic acid, piperidine/toluene-acetonitrile.

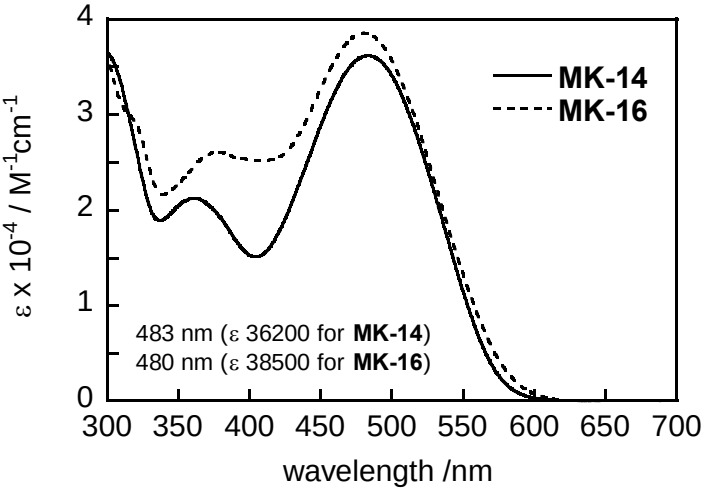

Figure 7. UV-vis spectra of **MK-14** (solid line) and **MK-16** (dotted line) in 20%THF-toluene

4-2. Photovoltaic Performances of DSSCs based on Substituted Carbazole Dyes

The action spectra of incident photo-to-current conversion efficiency (IPCE) for DSSCs based on **MK-14** and **MK-16** described in Figure 8. As well as the absorption properties of these dyes, the onset wavelengths of DSSCs were shifted to longer wavelength compared with those of **MK-1** and **MK-2**. IPCE values more than 70% were observed in the range of 400 to 650 nm with a maximum value of 83% at 530 nm for the DSSC based on **MK-14**, while the maximum values for **MK-16** were slightly decreased.

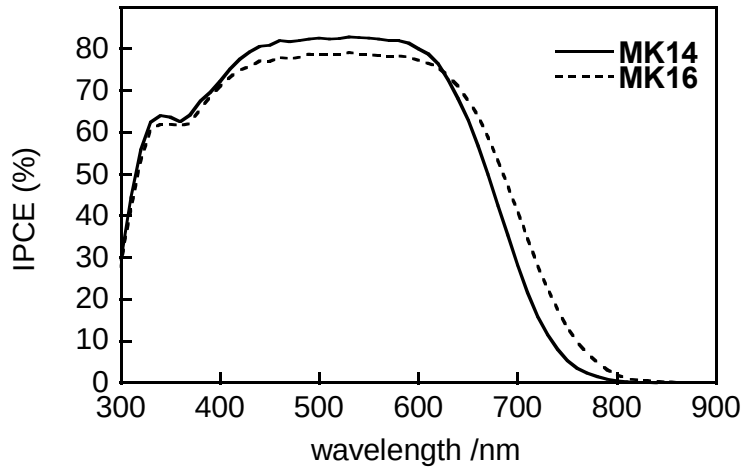

Figure 8. IPCE spectra of DSSCs with **MK-14** (solid line) and **MK-16** (dotted line).

Table 3. Photovoltaic Performances[a] of DSSCs based on **MK-14** and **MK-16**.

Dye	J_{SC} / mW cm^{-2}	V_{OC} / V	FF	η / %
MK-14	13.1	0.77	0.62	6.3
MK-16	12.6	0.76	0.59	5.6
N719	10.3	0.79	0.77	6.3
MK-14[b]	16.0	0.71	0.71	8.1

[a] Incident light: AM 1.5G (100 mW cm^{-2}) with a mask and without an anti-reflection film, TiO_2 electrode: 6 μm, Cell area: 0.2354 cm^2, Electrolyte: 0.6 M DMPImI + 0.1 M LiI + 0.05 M I_2 + 0.5 M TBP in acetonitrile, [b] TiO_2 electrode: 16 μm, Cell area: 0.2354 cm^2, Electrolyte: 0.6 M DMPImI + 0.1 M LiI + 0.2 M I_2 + 0.5 M TBP in acetonitrile.

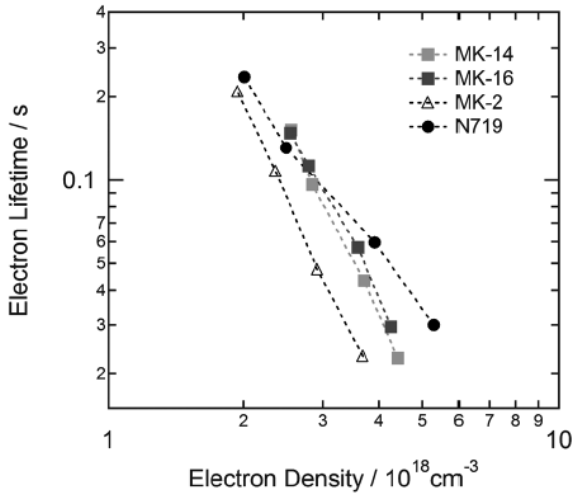

Figure 9. Electron lifetime in DSSCs with MK dyes and N719 as a function of electron density in DSSCs.

The photovoltaic performances of the DSSCs employing **MK-14** and **-16** with a thin-film TiO_2 electrode (6 μm) are summarized in Table 3, including the data from **N719** (a Ru complex dye). Note that higher V_{OC} (0.76-0.77 V) for the DSSCs based on **MK-14** and **MK-16** were observed in comparison to those (0.70-0.72 V) with **MK-1** and **MK-2** (Table 2). The values were quite close to that with **N719** dye (0.79 V). The J_{SC} values for the DSSCs based on **MK-14** and **MK-16** were almost equal or even better than that of **MK-2**. On the other hand, fill factor (*FF*) was decreased. The molecular size of MK dyes is larger than that of **N719**, and thus, its influence on the diffusion of redox couple would be expected. In order to fabricate highly efficient DSSCs, we prepared the DSSCs with thicker TiO_2 films to absorb more light and with an electrolyte containing higher concentration of I_3^- to increase the conductivity of the

electrolytes, increases of J_{SC} and *FF* were obtained. The maximum η value of 8.1% for **MK-14** was obtained under AM 1.5 G irradiation (100 mW cm^{-2}) with the electrolyte: 0.5 M DMPImI + 0.1 M LiI + 0.2 M I_2 + 0.5 M TBP in acetonitrile, and with an aperture mask and without antireflection film. Figure 9 shows the electron lifetime of the DSSCs with MK dyes and N719. The electron lifetime in the DSSCs with **MK-14** and **MK-16** were improved from that of the DSSC/**MK-2**, which was really closed to that of the DSSC with N719 ruthenium dye. This result indicates that the charge recombination could be retarded by the additional steric repulsion caused by the substituent on the carbazole moiety.

4-3. Molecular Design and Synthesis of Indolo[3,2-*b*]carbazole Dyes[16] and Thieno[3,2-*b*]indole Dyes[17]

As discussed above, the donor ability of the carbazole moiety increased by attaching the electron donating group at 3-position could cause to improve the absorption properties of dyes at the longer wavelength, hence increase J_{SC} of DSSCs with MK dyes, whereas fill factor was decreased by the large size of dye molecules. Then, we next designed the donor parts of dyes without any substituents, which were indolo[3,2-*b*]carbazole and thieno[3,2-*b*]indole moieties, to improve the photovoltaic performances of DSSCs based on these dyes. Indolo[3,2-*b*]carbazole derivatives were demonstrated as hole-transporting organic materials in fields of organic thin-film transistor and organic light-emitting diodes.[18] The molecular structure of indolo[3,2-*b*]carbazole have two nitrogen atoms in the aromatic plain on which alkyl chains can be added to enhance the solubility of the materials. We envisioned that indolo[3,2-*b*]carbazole unit could act as an efficient electron donor, and in the similar donor-p-acceptor structure, may have stronger electron donating ability, which could lead to red shift of absorption spectrum, than carbazole unit. Thieno[3,2-*b*]indole's structure is based on the indole moiety in which a thiophene ring, instead of a second benzene ring, is fused onto the five-membered ring at the 2-3 position of the indole, while organic dyes based on thieno[3,2-*b*]indole moiety has been little studied so far. The stronger electron donating ability of thieno[3,2-*b*]indole could be supposed than that of the corresponding carbazole because of the additional thiophene ring. Therefore, when the thieno[3,2-*b*]indole moiety could be introduced as a donor into the π-conjugated dye structure, a red-shift of the absorption spectra of the dyes could be expected. Furthermore, the planarity between thieno[3,2-*b*]indole moiety and oligothiophene linkage would be more increased for the dye molecule based on a thieno[3,2-*b*]indole donor part instead of a carbazole, which would cause the enhancement of the molar extinction coefficient (ε). The dye structures of dyes, **MKZ-21, MKZ-22**, **MKZ-39**, **MKZ-40**, and **MKZ-41**, with indolo[3,2-*b*]carbazole and thieno[3,2-*b*]indole moieties are described in Figure 10, and the synthetic procedures of these dyes are shown in Scheme 4 and 5.

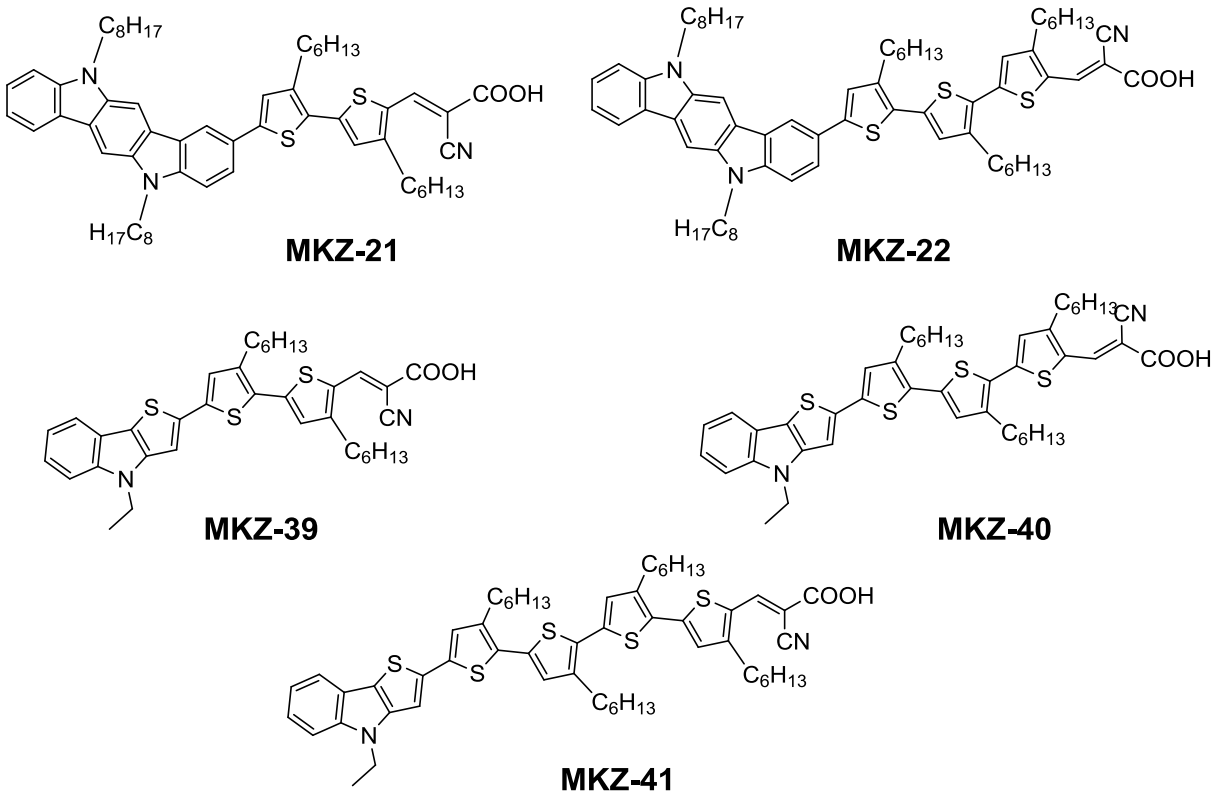

Figure 10. Molecular structures of MKZ dyes with indolo[3,2-*b*]carbazole and thieno[3,2-*b*]indole.

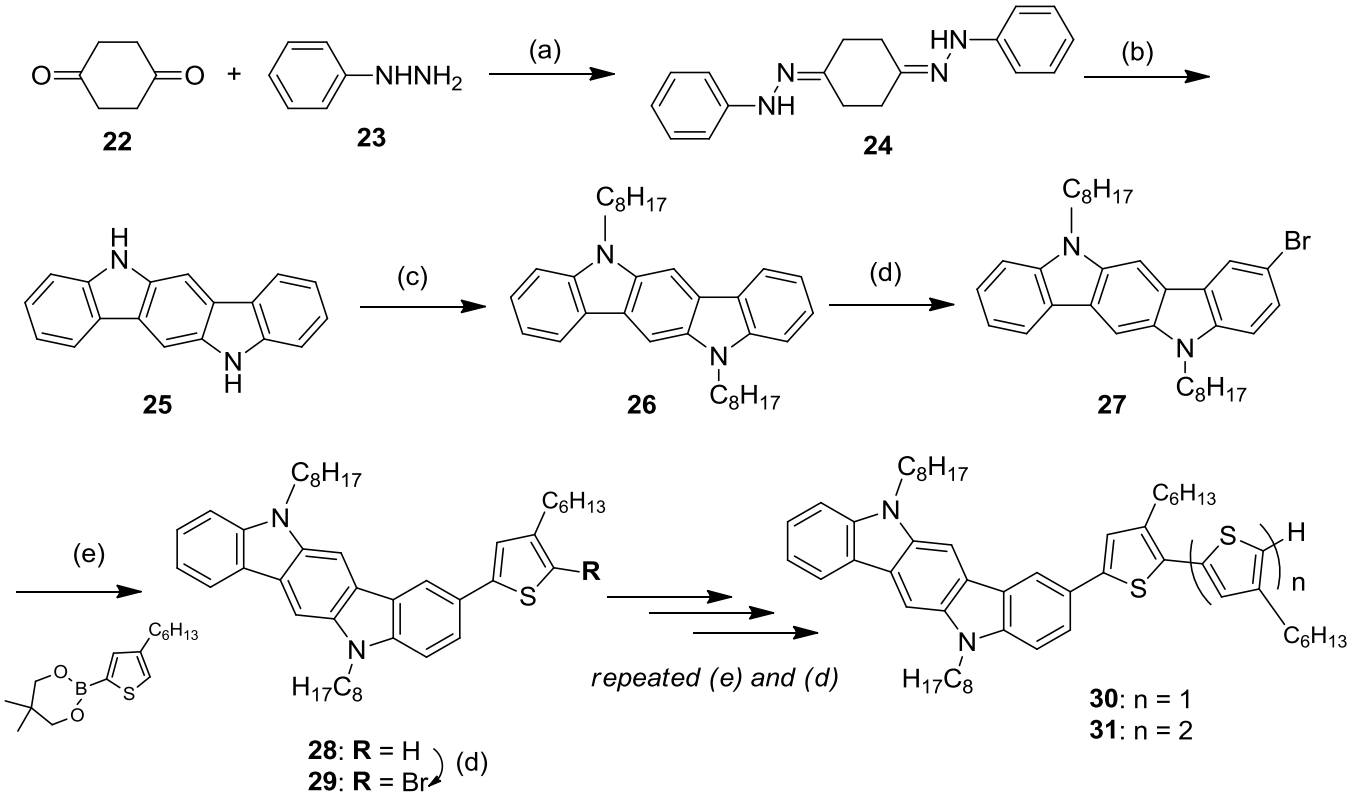

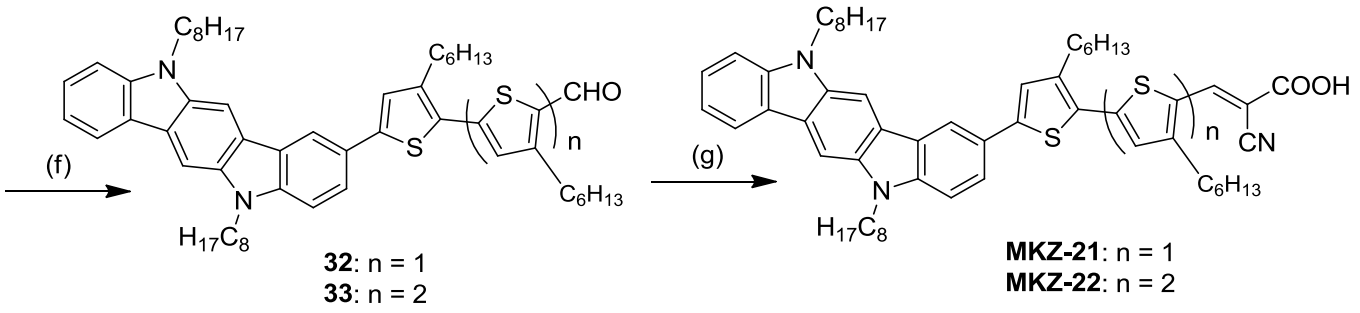

Scheme 4. Syntheses of **MKZ-21** and **MKZ-22**; (a) AcOH/EtOH; (b) conc. H_2SO_4; (c) 1-bromooctane, 50% NaOHaq, benzyltriethylammonium chloride/DMSO; (d) NBS/THF; (e) 5,5'-dimethyl-2-(4-*n*-hexylthiophen-2-yl)-1,3,2-dioxaborinane, $Pd(PPh_3)_4$, Na_2CO_3aq/DME; (f) $POCl_3$-DMF/DMF; (g) cyanoacetic acid, piperidine/toluene-acetonitrile.

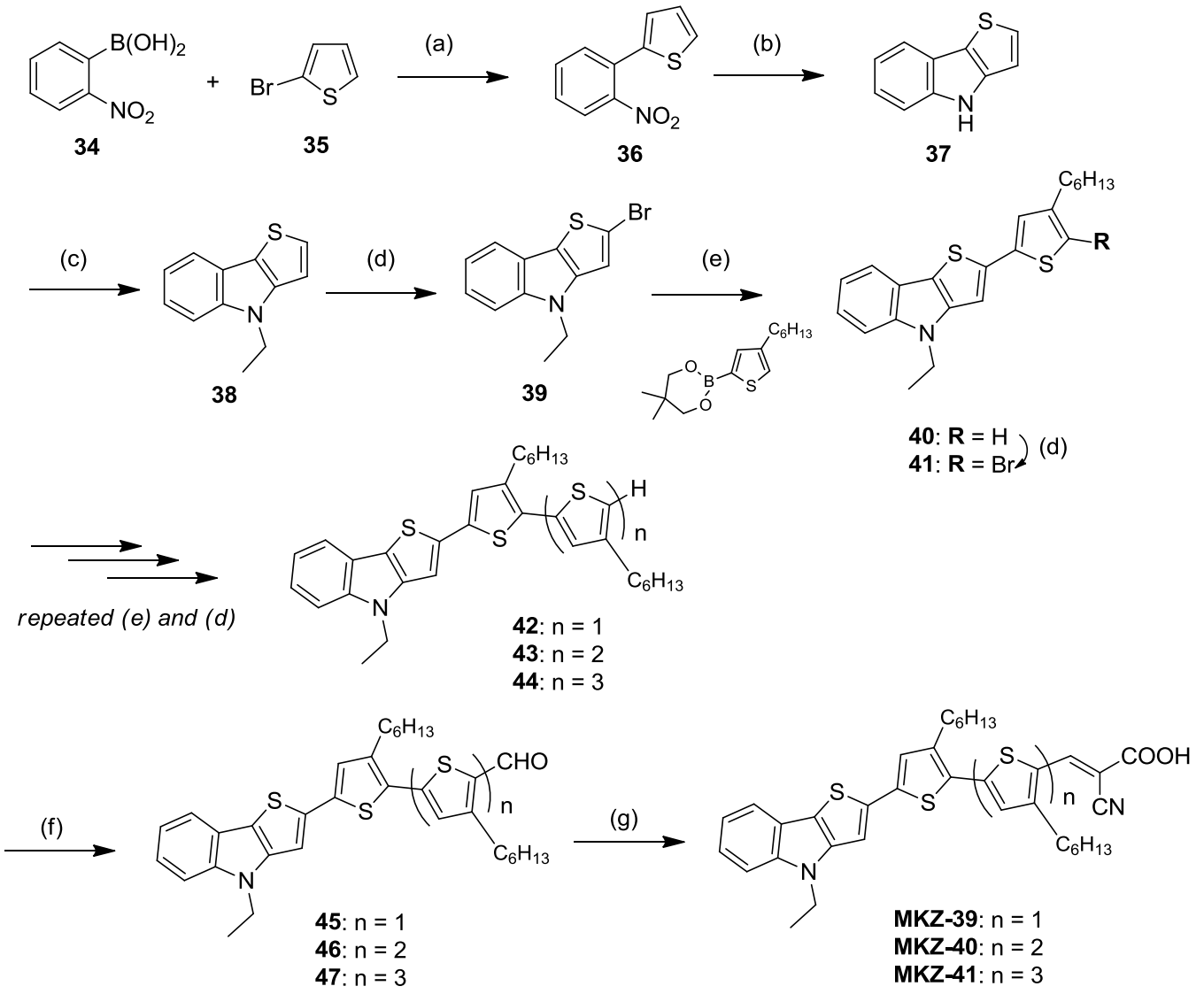

Scheme 5. Syntheses of **MKZ-39**, **MKZ-40**, and **MKZ-41**; (a) $Pd(PPh_3)_4$, Na_2CO_3aq/DME; (b) $P(OEt)_3$; (c) 1-bromoethane, aq 50% NaOH, benzyltriethylammonium chloride/DMSO; (d) NBS/THF; (e) 5,5'-dimethyl-2-(4-*n*-hexylthiophen-2-yl)-1,3,2-dioxaborinane, $Pd(PPh_3)_4$, Na_2CO_3aq/DME; (f) $POCl_3$-DMF/DMF; (g) cyanoacetic acid, piperidine/toluene-acetonitrile.

4-4. Absorption and Electrochemical Properties of MKZ Dyes

Figure 11 shows absorption spectra of these **MKZ** dyes in toluene solution. Both spectra of **MKZ-21** and **MKZ-22** exhibit two major prominent absorption bands, appearing at 310–360 nm and 450–560 nm, due to the π-π* transitions of the conjugated molecule, while the absorption spectra of **MKZ-39**, **MKZ-40**, and **MKZ-41** exhibit their major absorption band in the range of 400-600 nm in visible region, which mainly originate from the π-π* charge transfer transition. As expected, the molar extinction coefficient of thieno[3,2-*b*]indole dyes, **MKZ-39**, **MKZ-40**, and **MKZ-41**, at the maximum absorption was ranging from 43000 to 46000 M^{-1} cm^{-1}, which is a little higher than those of MK dyes in previous section, due to the less-twisted single bond between thieno[3,2-*b*]indole and first thiophene ring. The absorption and electrochemical properties of these dyes are summarized in Table 4. The oxidation potentials of the two sensitizers were measured with cyclic voltammetry (Table 1), the excited state oxidation potentials (E_{ox}^{*}) of **MKZ**-dyes are much more negative than the conduction band edge of TiO_2, which is located at –0.5 V (*vs*. NHE), and the ground state oxidation potentials (E_{ox}) of **MKZ**-dyes are sufficiently more positive than the iodine redox potential value (~0.4 V, *vs*. NHE), thus providing a thermodynamic driving force for the efficient electron injection to TiO_2 and the dye regeneration reaction from iodine redox.

Table 4. Absorption and electrochemical properties of MKZ dyes

Dye	λ_{max}[a] /nm (ε /M^{-1} cm^{-1})	λ_{max}[b] /nm (on TiO_2)	E_{ox}[c] (V vs NHE)	gap[d] (V)	E_{red}[e] (V vs NHE)
MKZ-21	492 (36,000)	429	0.84	2.03	–1.19
MKZ-22	501 (29,900)	437	0.93	1.85	–0.92
MKZ-39	502 (43,000)	451	1.01	1.97	–0.96
MKZ-40	496 (45,000)	458	0.89	1.89	–1.00
MKZ-41	490 (46,000)	466	0.83	1.84	–1.01

[a] UV-vis spectrum of each dye was measured in toluene solution through a 1 mm cell. [b] TiO_2 thickness ca. 1.5 μm. [c] Oxidation potentials of the dyes adsorbed on the TiO_2 films were measured under the following conditions: dye-adsorbed TiO_2 electrode (thickness: ca. 1.5 μm) as the working electrode, a Pt counter electrode, and a Ag/Ag^{+} reference electrode. [d] Estimated from the onset wavelength of the absorption spectrum of dye-adsorbed TiO_2 electrode. [e] Calculated from the equation: $E_{red} = E_{ox} - gap$.

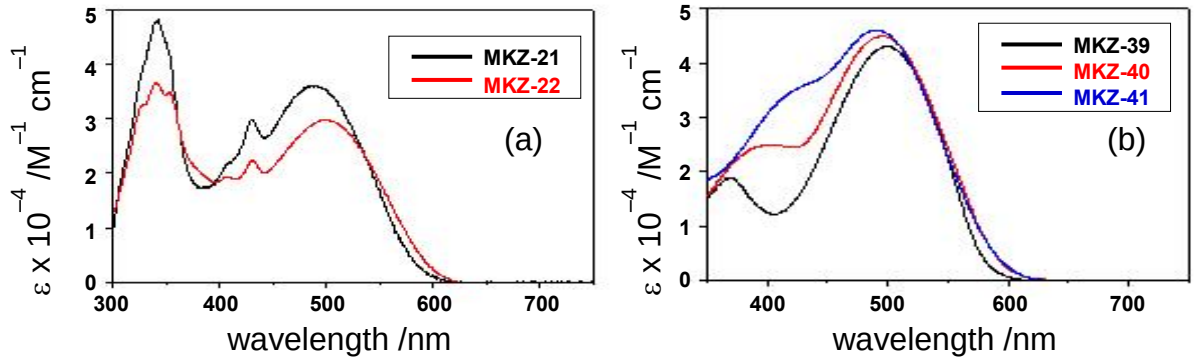

Figure 11. (a) UV-vis spectra of **MKZ-21** and **MKZ-22** in toluene; (b) UV-vis spectra of **MKZ-39**, **MKZ-40**, and **MKZ-41** in toluene.

4-5. Photovoltaic Performances of DSSCs based on MKZ Dyes.

The optimized IPCE spectra for **MKZ-21** and **MKZ-22** exhibit a plateau higher than 70% in the range from 420 to 620 nm with a maximal value of 83% at 500 nm for the DSSC based on **MKZ-21** as described in Figure 12(a). The optimized IPCE data of DSSCs based on **MKZ-39**, **MKZ-40**, and **MKZ-41** are depicted in Figure 12(b), which have a plateau region higher than 60% in the range from 400 to 650 nm with a maximal value of 74% at 490 nm for the DSSC/**MKZ-40**. In both cases of indolo[3,2-*b*]carbazole and thieno[3,2-*b*]indole dyes, with increasing the number of the thiophene unit, the IPCE spectra were gradually shifted to red region because of the extended π-conjugation system. The onset wavelength of IPCE spectra was shifted to longer wavelength than the unsubstituted carbazole dyes, **MK-1** and **MK-2**, corresponding to the same number of thiophene, due to the higher donor ability than unsubstituted carbazole moiety. However, the lower IPCE value of the DSSC/**MKZ-22** was observed than that of **MKZ-21**, as well as the case of DSSC/**MKZ-41** compared to DSSCs/**MKZ-39** and **MKZ-40**.

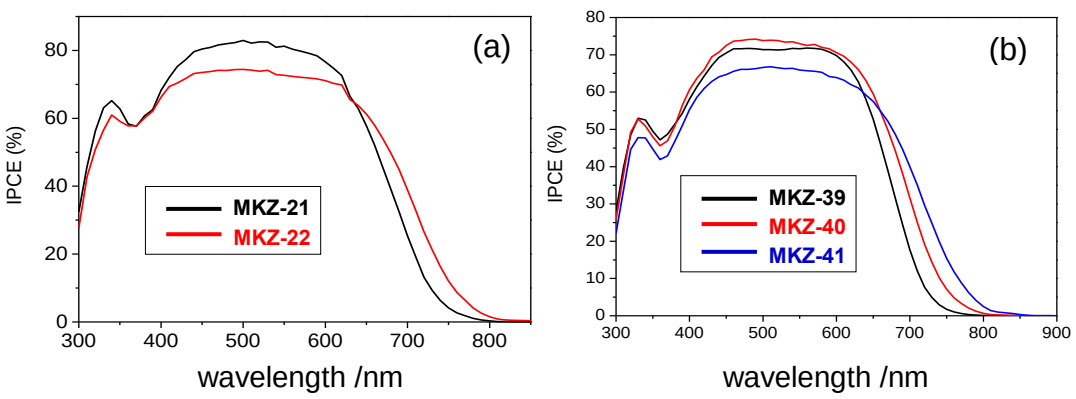

Figure 12. (a) Optimized IPCE spectra of DSSCs/**MKZ-21** and **MKZ-22**; (b) Optimized IPCE spectra of DSSCs/**MKZ-39**, **MKZ-40**, and **MKZ-41**.

Photovoltaic performances of the DSSCs based on these indolo[3,2-*b*]carbazole and thieno[3,2-*b*]indole dyes are shown in Table 5. Under AM 1.5G irradiation, the DSSC/**MKZ-21** gave a J_{SC} of 15.4 mA cm^{-2}, a V_{OC} of 0.71 V, a *FF* of 0.67, corresponding to an overall conversion efficiency (η) of 7.3%, while under the same conditions, the **MKZ-22** sensitized solar cell gave a J_{SC} of 15.5 mA cm^{-2}, a V_{OC} of 0.70 V, a *FF* of 0.62, corresponding to a η of 6.7%. The slightly larger J_{SC} of the DSSC/**MKZ-22** as compared to the DSSC/**MKZ-21** demonstrates the beneficial influence of the red-shifted absorption spectrum of **MKZ-22** on TiO_2 film and the broadening of the IPCE spectrum of the DSSC/**MKZ-22**. However, the lower *FF* of the DSSC/**MKZ-22**, probably due to the larger molecular size of **MKZ-22** than **MKZ-21**, finally led to the lower conversion efficiency of the DSSC/**MKZ-22**. This phenomenon was similarly observed as the case of **MK-14** and **MK-16** discussed in the section 4-2. It is considered that the additional substituent on the carbazole moiety or the large size of donor moiety may strongly affects the diffusion of redox couple in the electrolyte compared with the unsubstituted carbazole dyes, **MK-1** and **MK-2**. The DSSC/**MKZ-40** gave the best photovoltaic performance, with a J_{SC} of 14.6 mA cm^{-2}, a V_{OC} of 0.70 V, a *FF* of 0.76, and a η of 7.8%. J_{SC} increased in order of **MKZ-41** > **MKZ-40** > **MKZ-39** as the result of the broadening of the IPCE spectra with the increasing number of the thiophene unit. However, V_{OC} of the DSSC/**MKZ-41** is slightly lower than those of DSSCs/**MKZ-39** and **MKZ-40**.

Table 5. Photovoltaic Performances[a] of DSSCs based on **MKZ-21**, **MKZ-22**, **MKZ-39**, **MKZ-40**, and **MKZ-41**.

Dye	J_{SC} / mW cm^{-2}	V_{OC} / V	*FF*	η / %
MKZ-21	15.4	0.71	0.67	7.3
MKZ-22	15.5	0.70	0.62	6.7
MKZ-39	13.8	0.70	0.77	7.4
MKZ-40	14.6	0.70	0.76	7.8
MKZ-41	15.0	0.66	0.74	7.3

[a] Incident light: AM 1.5G (100 mW cm^{-2}) with a mask and without an anti-reflection film, TiO_2 electrode: 14 μm, Cell area: 0.2354 cm^2, Electrolyte: 0.6 M DMPImI + 0.1 M LiI + 0.2 M I_2 + 0.5 M TBP in acetonitrile.

5. CARBAZOLE DYES WITH FLUOROALKYL GROUP ON OLIGOTHIOPEHENE LINKAGE[19]

5-1. Synthesis

One of the most efficient function of alkyl group on the oligothiophene linkage is its hydrophobicity which contributes the durability of DSSCs because the desorption of dye-molecules from the TiO_2 surface often occur by the water contamination. MK dyes with alkyl groups on the thiophene linkage have such function to prevent water from approaching to the interface between dye and TiO_2 surface. To enhance the hydrophobicity of organic dyes, we designed and synthesized MK dyes (**MK-53**, **MK-54**, and **MK-55**) introducing the fluorinated alkyl groups on the oligothiophene linkage instead of normal alkyl chains (Figure 13). Fluorine atoms are located to be apart from the oligothiophene moiety with an alkyl spacer group because the electron withdrawing effect of fluorine atom might influence the electronic feature of π-conjugated system of dyes. Synthesis of these dyes were accomplished by the iterative Pd-catalyzed C-H arylation and halogen exchange reaction and/or the repeated Suzuki coupling and bromination reaction, Vilsmeiyer reaction, and Knoevenagel condensation, which described in Scheme 6 and 7.

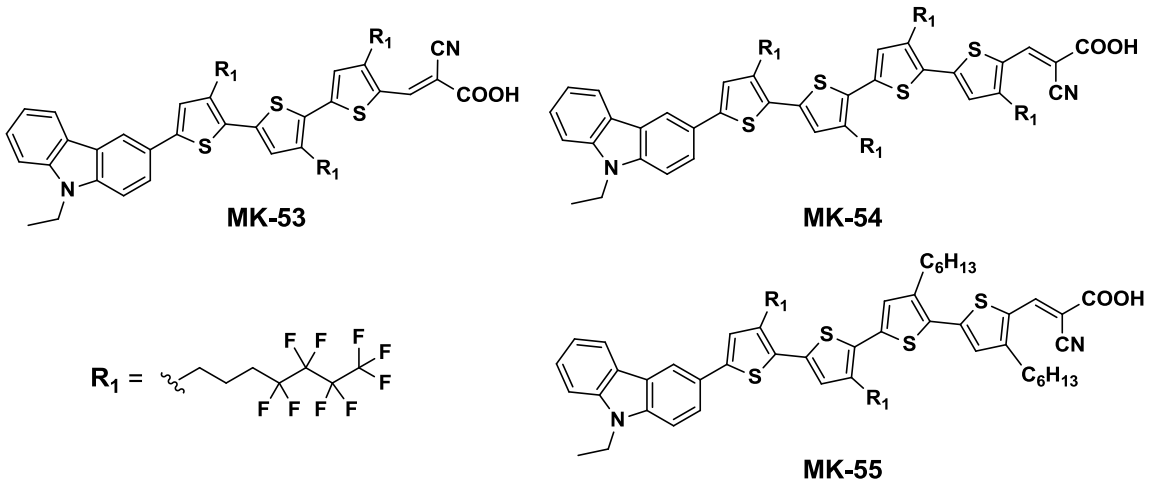

Figure 13. Molecular structures of MK dyes with fluorinated alkyl groups, **MK-53**, **MK-54**, and **MK-55**.

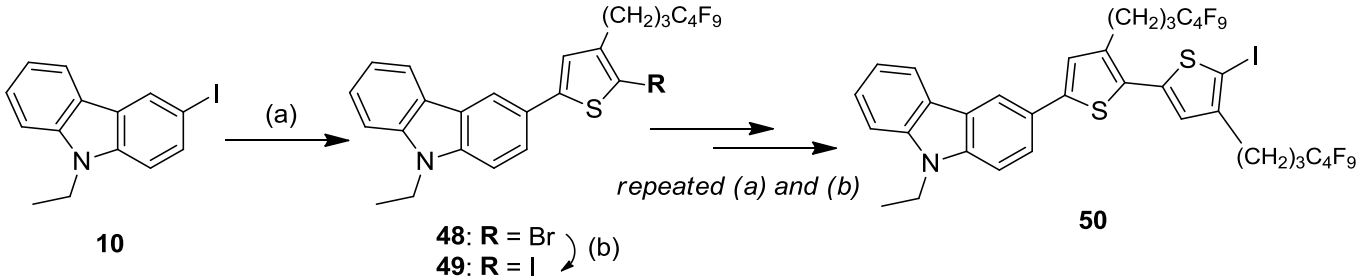

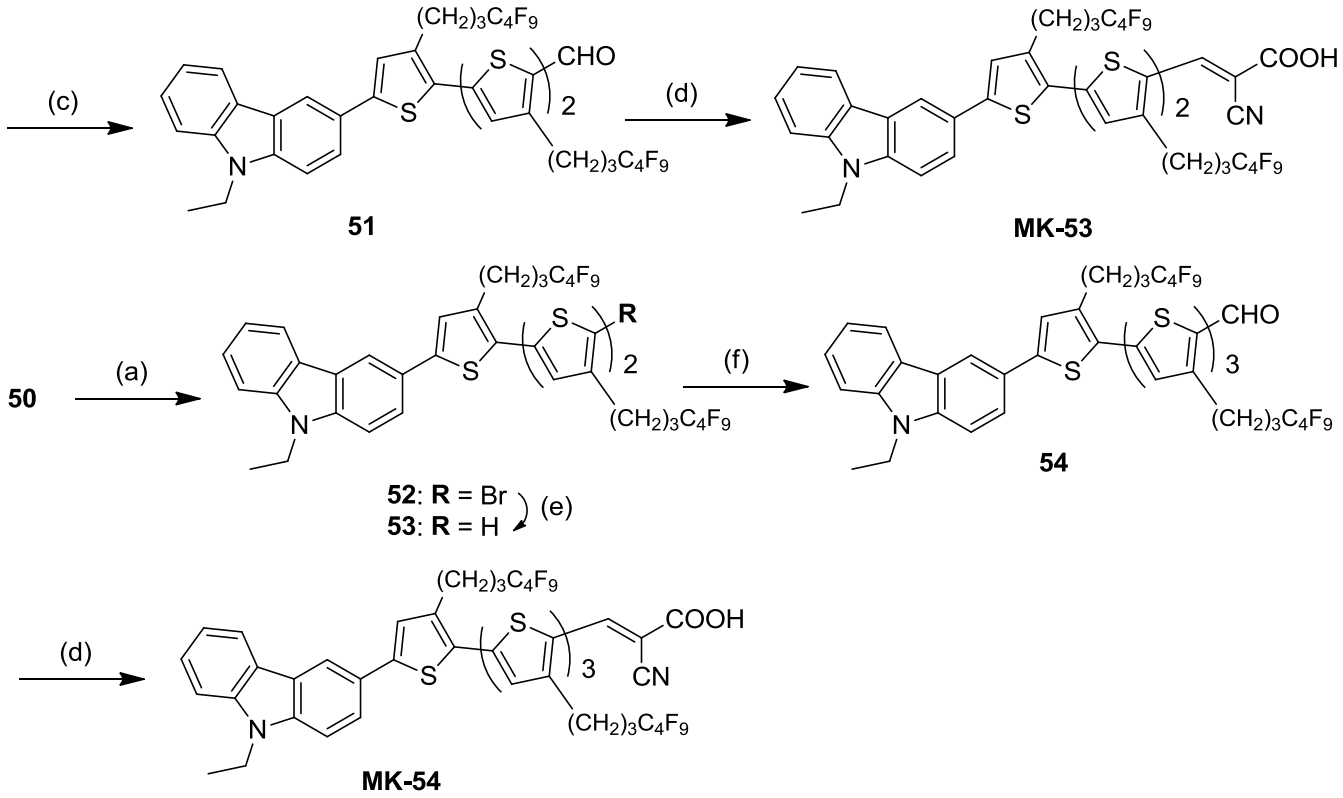

Scheme 6. Synthesis of **MK-53** and **MK-54** by the iterative Pd-catalyzed CH arylation and halogen exchange reaction; (a) 2-bromo-3-(4,4,5,5,6,6,7,7,7-nonafluoroheptyl)thiophene, $PdCl_2(PPh_3)_2$, $AgNO_3$, KF/DMSO; (b) *n*-BuLi, I_2/THF; (c) 3-(4,4,5,5,6,6,7,7,7-nonafluoroheptyl)-2-thiophenecarbaldehyde, $PdCl_2(PPh_3)_2$, $AgNO_3$, KF/DMSO; (d) cyanoacetic acid, piperidine/toluene-acetonitrile; (e) *n*-BuLi, MeOH/THF; (f) 5-iodo-3-(4,4,5,5,6,6,7,7,7-nonafluoroheptyl)-2-thiophenecarbaldehyde, $PdCl_2(PPh_3)_2$, $AgNO_3$, KF/DMSO.

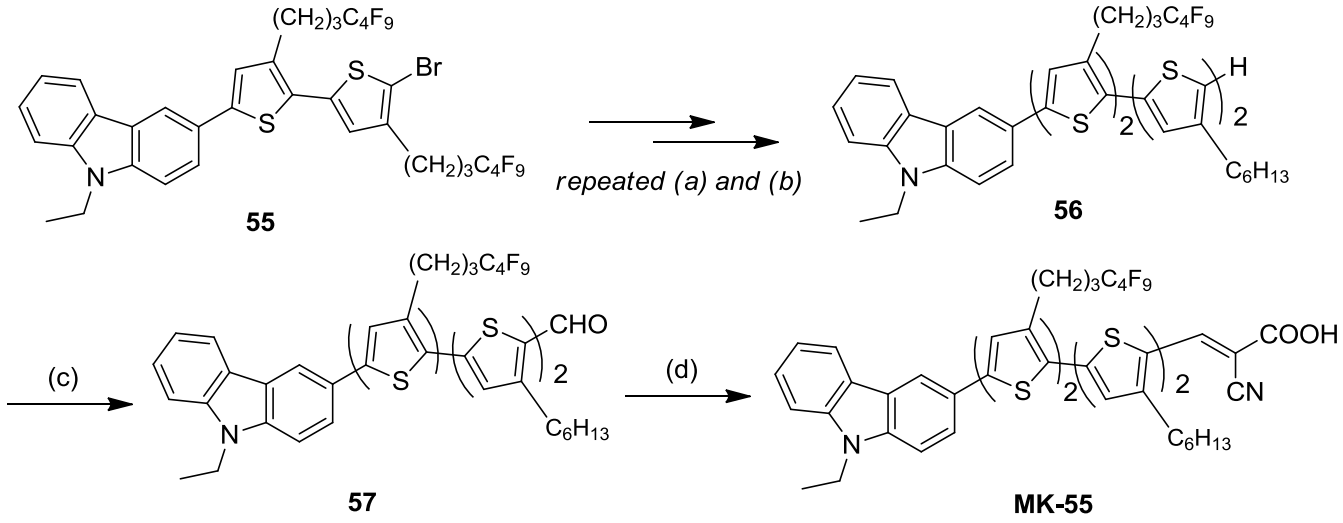

Scheme 7. Synthesis of **MK-55** by the repeated Suzuki coupling and bromination reaction; (a) 5,5'-dimethyl-2-(4-*n*-hexylthiophen-2-yl)-1,3,2-dioxaborinane, $Pd(PPh_3)_4$, Na_2CO_3aq/DME; (b) NBS/THF; (c) $POCl_3$-DMF/DMF; (d) cyanoacetic acid, piperidine/toluene-acetonitrile.

5-2. Absorption properties of Fluorinated Dyes and Photovoltaic Performances of DSSCs

The absorption spectra of **MK-53**, **-54**, and **-55** were shown in Figure 14. In all cases the blue shift of absorption spectra of these dyes were observed. In addition, the molar absorption coefficients of **MK-53** (31800) and **MK-54** (32500) were lower than those of **MK-1** and **MK-2** (about 38000). Furthermore, the onsets of the UV-vis spectra of these dyes are indicated at the similar wavelength even in the different number of thiophene. On the other hand, the chemical shifts (141.1, 127.9, 126.0, 120.8 ppm) in ^{13}C NMR of thiophene ring of 3-nonafluoroheptylthiophene monomer was almost identical with those (143.2, 128.3, 125.0, 119.7 ppm) of the *n*-hexylthiophene monomer. This result indicates that the electron negative effect of fluorine atoms in the fluoroalkyl chains on the thiophene ring can be neglected because of the existence of the propyl spacer between thiophene ring and fluoroalkyl group. Therefore, the drastic changes of UV-vis spectra of **MK-53**, **MK-54**, and **MK-55** were not related to the existence of fluoroalkyl chains but other factors such as solvent effect and so on. As expected, the solubility of these fluorinated dyes in toluene became worse than dyes with normal alkyl chains. Therefore, 10% of tetrahydrofuran included toluene solution of these dyes was also applied for dye-adsorption on the TiO_2 nanoparticles. The photovoltaic performances of DSSCs employing these dyes are depicted in Table 6, including the data of a DSSC based on **MK-2**. Although the J_{SC} values of the DSSCs with **MK-53**, **MK-54**, and **MK-55** were all lower than that of a DSSC/**MK-2**, corresponding to the absorption properties, the V_{OC} of the DSSCs with **MK-53** and **MK-55** were slightly improved in comparison to that of a DSSC based on **MK-2**, probably due to not only the steric blocking but also the electronic repulsion by fluoroalkyl groups instead of alkyl chains. However, The relatively low V_{OC} of a DSSC/**MK-54**, which has a quaterthiophene with fluroalkyl chains as a linker, was observed. In the case of 10%THF-toluene solution of these dyes used for the dye-adsorption, both J_{SC} and V_{OC} were drastically decreased. This is probably because of the reduced dye-adsorption amount on TiO_2 surface. The DSSC/**MK-55** gave the best photovoltaic performance, with a J_{SC} of 11.8 mA cm^{-2}, a V_{OC} of 0.76 V, a *FF* of 0.73, and a η of 6.5% under one-sun condition, which was even better performance than that of a DSSC/**MK-2**, using the thin-film TiO_2 electrode (~7 μm).

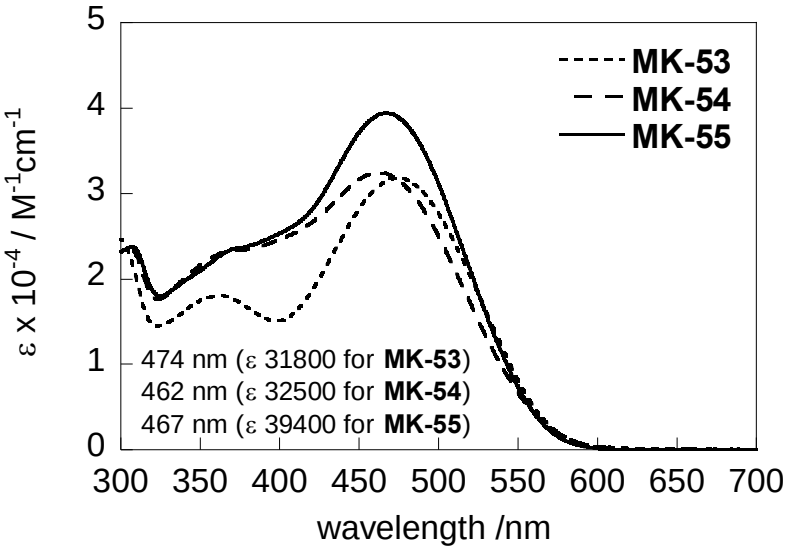

Figure 14. UV-vis spectra of **MK-53** (dotted line), **MK-54** (dashed line), and **MK-55** (solid line) in 20%THF-toluene

Table 6. Photovoltaic Performances[a] of DSSCs based on **MK-2**, **MK-53**, **MK-54**, and **MK-55**

Dye	solvent	J_{SC} / mW cm^{-2}	V_{OC} / V	FF	η / %
MK-2	toluene [b]	12.2	0.74	0.71	6.3
MK-53	toluene [c]	9.7	0.75	0.76	5.5
MK-53	10%THF-toluene [b]	8.3	0.68	0.76	4.2
MK-54	toluene [c]	8.3	0.71	0.75	4.4
MK-54	10%THF-toluene [b]	4.8	0.61	0.74	2.2
MK-55	toluene [b]	11.8	0.76	0.73	6.5
MK-55	10%THF-toluene [b]	8.6	0.69	0.76	4.4

[a] Incident light: AM 1.5G (100 mW cm^{-2}) with a mask and without an anti-reflection film, TiO_2 electrode: 7 μm, Cell area: 0.2354 cm^2, Electrolyte: 0.6 M DMPImI + 0.1 M LiI + 0.2 M I_2 + 0.5 M TBP in acetonitrile, [b] solution, [c] partial solution.

6. CONCLUSIONS

We have developed several organic dyes based on carbazole and carbazole derivative donor structures and oligothiophene moiety having long alkyl chains, which are useful for the sensitizers of DSSCs. These dyes were designed to act as not only sensitizers but also functional materials on the TiO_2 surface due to the hydrophobic alkyl chains on the oligothiophene linkage. The remarkable feature of these dyes is the blocking effect by the long alkyl chains to retard the electron recombination from TiO_2 to the electrolyte,

thereby high open circuit voltage of DSSCs. The DSSCs based on MK dyes showed high photovoltaic performance of up to 8% under AM 1.5G irradiation and good long-term stability under continuous simulated visible light irradiation. It was also found that the molecular stability of these dyes under illumination was quite improved because of the delocalization of dye-cations on the oligothiophene moiety. Recently, organic dyes with high blocking effect have been attracted much attention for the sensitizers of DSSCs based on cobalt redox system.[5,20] The DSSCs with cobalt redox system show much higher open circuit voltage (~ 1.0 V) than that of DSSCs with iodine redox system and, but the rate of the charge recombination of the injected electron in the TiO_2 to the cobalt redox is much faster than the case of iodine redox. Therefore, these bulky alkyl-functionalized organic dyes are useful for DSSCs based on cobalt redox system to retard the charge recombination rate. Moreover, organic dyes are used as co-adsorptions with various complex dyes (ruthenium,[21] porphrin,[5] and phthalocyanine[22]) to cover their weak absorption regions with high molar extinction coefficient of organic dyes. Our approach toward efficient molecular photovoltaics based on organic dye sensitizers strongly indicates the next molecular design and multiple usages of organic dyes corresponding to various types of DSSCs. To improve the photovoltaic performance of the DSSCs, it is significantly necessary to consider the interaction between dye materials and other materials, such as substrates, TiO_2 nanoparticles, redox species, electrolyte, additives, counter electrode and so on. Therefore, we, synthetic chemist, need to observe the phenomena of photovoltaic performances carefully and discuss it deeply with other professional scientists in the field of device chemistry, spectroscopic analysis and so on, to design the next generation of materials for dye-sensitized solar cells.

ACKNOWLEDGEMENTS

We acknowledged financial support from the New Energy and Industrial Technology Development Organization (NEDO) of Japan. We greatly thank to Prof. Z.S. Wang (currently FuDan University), Dr. X.-H. Zhang, Ms. Y. Cui, who had also been engaged in these works with us. We also thank Prof. S. Mori (Shinshu University), Prof. A. Mori (Kobe University), Prof. R. Kato (Nihon University), Dr. A. Furube and Dr. T. N. Murakami (AIST) to collaborate on these works.

REFERENCES

1. G. Smestad, C. Bignozzi, and R. Argazzi, *Sol. Energy Mater. Sol. Cells*, 1994, **32**, 259; A. Kay and M. Grätzel, *Sol. Energy. Mater. Sol. Cells*, 1996, **44**, 99; A. Hagfeldt and M. Grätzel, *Acc. Chem. Res.*, 2000, **33**, 269; A. Hagfeldt, G. Boschloo, L. Sun, L. Kloo, and H. Pettersson, *Chem. Rev.*, 2010, **110**, 6595.

2. B. O'Regan and M. Grätzel, *Nature*, 1991, **353**, 737.
3. M. K. Nazeeruddin, F. De Angelis, S. Fantacci, A. Selloni, G. Viscardi, P. Liska, S. Ito, B. Takeru, and M. Grätzel, *J. Am. Chem. Soc.*, 2005, **127**, 16835; Y. Chiba, A. Islam, Y. Watanabe, R. Komiya, N. Koide, and L. Han, *Jpn. J. Appl. Phys.*, 2006, **45**, L638; Y. Cao, Y. Bai, Q. Yu, Y. Cheng, S. Liu, D. Shi, F. Gao, and P. Wang, *J. Phys. Chem. C*, 2009, **113**, 6290.
4. Y. Kijitori, M. Ikegami, and T. Miyasaka, *Chem. Lett.*, 2007, **36**, 190; T. Miyasaka, M. Ikegami, and Y. Kijitori, *J. Electrochem. Soc.*, 2007, **154**, A445.
5. A. Yella, H. Lee, H. N. Tsao, C. Yi, A. K. Chandiran, M. K. Nazeeruddin, E. W. Diau, C. Yeh, S. M. Zakeeruddin, and M. Grätzel, *Science*, 2011, **334**, 629.
6. M. K. Nazeeruddin, S. M. Zakeeruddin, R. Humphry-Baker, M. Jirousek, P. Liska, N. Vlachopoulos, V. Shklover, C.-H. Fischer, and M. Grätzel, *Inorg. Chem.*, 1999, **38**, 6298.
7. M. K. Nazeeruddin, S. M. Zakeeruddin, J.-J. Lagref, P. Liska, P. Comtea, C. Barolo, G. Viscardi, K. Schenk, and M. Grätzel, *Coordination Chem. Rev.*, 2004, **248**, 1317.
8. M. K. Nazeeruddin, P. Péchy, and M. Grätzel, *Chem. Commun.*, 1997, 1705.
9. R. K. Kanaparthi, J. Kandhadi, and L. Giribabu, *Tetrahedron*, 2012, **68**, 8383, references are therein; D. H. Lee, M. J. Lee, H. M. Song, B. J. Song, K. D. Seo, M. Pastore, C. Anselmi, S. Fantacci, F. De Angelis, M. K. Nazeeruddin, M. Grätzel, and H. K. Kim, *Dyes Pigments*, 2011, **91**, 192; Y. Bai, J. Zhang, D. Zhou, Y. Wang, M. Zhang, and P. Wang, *J. Am. Chem. Soc.*, 2011, **133**, 11442; G. Zhang, H. Bala, Y. Cheng, D. Shi, X. Lv, Q. Yu, and P. Wang, *Chem. Commun.*, 2009, 2198; D. P. Hagberg, J.-H. Yum, H.-J. Lee, F. D. Angelis, T. Marinado, K. M. Karlsson, R. Humphry-Baker, L. Sun, A. Hagfeldt, M. Grätzel, and M. K. Nazeeruddin, *J. Am. Chem. Soc.*, 2008, **130**, 6259; X. Yang, J.-K. Fang, Y. Suzuma, F. Xu, A. Orita, J. Otera, S. Kajiyama, N. Koumura, and K. Hara, *Chem. Lett.*, 2011, **40**, 620; X. Yang, S. Kajiyama, J.-K. Fang, F. Xu, Y. Uemura, N. Koumura, K. Hara, A. Orita, and J. Otera, *Bull. Chem. Soc. Jpn.*, 2012, **85**, 687; E. Miyazaki, T. Okanishi, Y. Suzuki, N. Ishine, H. Mori, K. Takimiya, and Y. Harima, *Bull. Chem. Soc. Jpn.*, 2010, **84**, 459; S. Mathew and H. Imahori, *J. Mater. Chem.*, 2011, **21**, 7166.
10. J. M. Rehm, G. L. McLendon, Y. Nagasawa, K. Yoshihara, J. Moser, and M. Grätzel, *J. Phys. Chem.*, 1996, **100**, 9577; K. Hara, T. Sato, R. Katoh, A. Furube, Y. Ohga, A. Shinpo, S. Suga, K. Sayama, H. Sugihara, and H. Arakawa, *J. Phys. Chem. B*, 2003, **107**, 597; K. Hara, Z.-S. Wang, T. Sato, A. Furube, R. Katoh, H. Sugihara, Y. Dan-oh, C. Kasada, A. Shinpo, and S. Suga, *J. Phys. Chem. B*, 2005, **109**, 15476; Z.-S. Wang, Y. Cui, K. Hara, Y. Dan-oh, C. Kasada, and A. Shinpo, *Adv. Mater.*, 2007, **19**, 1138; X. Ren, Q. Feng, G. Zhou, C.-H. Huang, and Z.-S. Wang, *J. Phys. Chem. C*, 2010, **114**, 7190.
11. T. Horiuchi, H. Miura, K. Sumioka, and S. Uchida, *J. Am. Chem. Soc.*, 2004, **126**, 12218; S. Ito, S. M.

Zakeeruddin, R. Humphry-Baker, P. Liska, R. Charvet, P. Comte, M. K. Nazeeruddin, P. Péchy, M. Takata, H. Miura, S. Uchida, and M. Gratzel, *Adv. Mater.*, 2006, **18**, 1202; S. Ito, H. Miura, S. Uchida, M. Takata, K. Sumioka, P. Liska, P. Comte, P. Péchy, and M. Gratzel, *Chem. Commun.*, 2008, 5194; Q. Li, L. Lu, C. Zhong, J. Shi, Q. Huang, X. Jin, T. Peng, J. Qin, and Z. Li, *J. Phys. Chem. C*, 2009, **113**, 14588; M. Akhtaruzzaman, A. Islam, F. Yang, N. Asao, E. Kwon, S. P. Singh, L. Han, and Y. Yamamoto, *Chem. Commun.*, 2011, 12400.

12. N. Koumura, Z. Wang, S. Mori, M. Miyashita, E. Suzuki, and K. Hara, *J. Am. Chem. Soc.*, 2006, **128**, 14256 (Additions and Corrections, 2008, **130**, 4202).
13. N. Masuda, S. Tanba, A. Sugie, D. Monguchi, N. Koumura, K. Hara, and A. Mori, *Org. Lett.*, 2009, **11**, 2297.
14. Z. Wang, N. Koumura, Y. Cui, M. Takahashi, H. Sekiguchi, A. Mori, T. Kubo, A. Furube, and K. Hara, *Chem. Mater.*, 2008, **20**, 3993.
15. N. Koumura, Z. Wang, M. Miyashita, Y. Uemura, H. Sekiguchi, Y. Cui, A. Mori, S. Mori, and K. Hara, *J. Mater. Chem.*, 2009, **19**, 4829.
16. X.-H. Zhang, Z.-S. Wang, Y. Cui, N. Koumura, A. Furube, and K. Hara, *J. Phys. Chem. C*, 2009, **113**, 13409.
17. X.-H. Zhang, Y. Cui, R. Katoh, N. Koumura, and K. Hara, *J. Phys. Chem. C*, 2010, **114**, 18283.
18. N.-X. Hu, S. Xie, Z. Popovic, B. S. Ong, and A.-M. Hor, *J. Am. Chem. Soc.*, 1999, **121**, 5097; S. Wakim, J. Bouchard, M. Simard, N. Drolet, Y. Tao, and M. Leclerc, *Chem. Mater.*, 2004, **16**, 4386; Y. Li, Y. Wu, S. Gardner, and B. S. Ong, *Adv. Mater.*, 2005, **17**, 849; Y. Wu, Y. Li, S. Gardner, and B. S. Ong, *J. Am. Chem. Soc.*, 2005, **127**, 614; Y. Li, Y. Wu, and B. S. Ong, *Macromolecules*, 2006, **39**, 6521; M. Belletête, N. Blouin, P.-L. T. Boudreault, M. Leclerc, and G. Durocher, *J. Phys. Chem. A*, 2006, **110**, 13696; P.-L. T. Boudreault, S. Wakim, N. Blouin, M. Simard, C. Tessier, Y. Tao, and M. Leclerc, *J. Am. Chem. Soc.*, 2007, **129**, 9125.
19. S. Tanba, A. Sugie, N. Masuda, D. Monguchi, N. Koumura, K. Hara, and A. Mori, *Heterocycles*, 2010, **82**, 505.
20. S. M. Feldt, E. A. Gibson, E. Gabrielsson, L. Sun, G. Boschloo, and A. Hagfeldt, *J. Am. Chem. Soc.*, 2010, **132**, 16714; M. Ohta, N. Koumura, K. Hara, and S. Mori, *Electrochem. Commun.*, 2011, **13**, 778; Y. Liu, J. R. Jennings, Y. Huang, Q. Wang, S. M. Zakeeruddin, and M. Grätzel, *J. Phys. Chem. C*, 2011, **115**, 18847; Y. Bai, J. Zhang, D. Zhou, Y. Wang, M. Zhang, and P. Wang, *J. Am. Chem. Soc.*, 2011, **133**, 11442; T. N. Murakami, N. Koumura, T. Uchiyama, Y. Uemura, K. Obuchi, N. Masaki, M. Kimura, and S. Mori, *J. Mater. Chem. A*, 2013, in press (DOI: 10.1039/c2ta00897a).
21. L. Han, A. Islam, H. Chen, C. Malapaka, B. Chiranjeevi, S. Zhang, X. Yang, and M. Yanagida, *Energy Environ. Sci.*, 2012, **5**, 6057; H. Ozawa, R. Shimizu, and H. Arakawa, *RSC Adv.*, 2012, **2**,

3198.

22. M. Kimura, H. Nomoto, N. Masaki, and S. Mori, *Angew. Chem. Int. Ed.*, 2012, **51**, 4371; M.-E. Ragoussi, J.-J. Cid, J.-H. Yum, G. de la Torre, D. Di Censo, M. Grätzel, M. K. Nazeeruddin, and T. Torres, *Angew. Chem. Int. Ed.*, 2012, **51**, 4375.

Dr. Nagatoshi Koumura recieved his Ph.D. degree from Tohoku University in 1999 under the direction of Professor Nobuyuki Harada. He has been a postdoctoral fellow in the group of Professor Ben L. Feringa at University of Groningen, The Netherlands, from 1999 to 2002. He then joined National Institute of Advanced Industrial Science and Technology (AIST) in Japan as a researcher. He is currently belonging to Research Center for Photovoltaic Technologies in AIST as a senior researcher. In 2008 he joined the Graduate School of Pure and Applied Science at University of Tsukuba as a cooperated associate professor. His research is mainly focused on organic synthesis and stereochemistry, and his current interest is the development of organic functional materials for molecular photovoltaics toward their practical use.

Dr. Kohjiro Hara obtained his Ph.D. degree from Tokyo Institute of Technology in 1997 under the direction of Professor Tadayoshi Sakata, and then joined the group of Dr. Hironori Arakawa in National Institute of Materials and Chemical Research (NIMC). From 2001, He was a researcher of National Institute of Advance Science and Technology (AIST) according to the reconstruction of the institute, and has been a senior researcher from 2008. His research interest is photoelectrochemistry, solar cells based on organic and inorganic materials, and photovoltaic device technologies.